A Raman scattering study of the phase transitions in $SrTiO_3$ and in the mixed system $(Sr_{1-x}Ca_x)TiO_3$ at ambient pressure from T = 300 K down to 8 K

2002 J. Phys.: Condens. Matter 14 2079

(http://iopscience.iop.org/0953-8984/14/8/333)

INSTITUTE OF PHYSICS PUBLISHING JOURNAL OF PHYSICS: CONDENSED MATTER

J. Phys.: Condens. Matter **14** (2002) 2079–2092 PII: S0953-8984(02)30907-X

A Raman scattering study of the phase transitions in $SrTiO_3$ and in the mixed system $(Sr_{1-x}Ca_x)TiO_3$ at ambient pressure from T = 300 K down to 8 K

R Ouillon[1], J-P Pinan-Lucarre[1], P Ranson[1], Ph Pruzan[1], Sanjay Kumar Mishra[2], Rajeev Ranjan[2] and Dhananjai Pandey[2,3]

[1] Physique des Milieux Condenses, UMR 7602, Universite Pierre et Marie Curie, B77, 4 Place Jussieu, 75252 Paris Cedex 05, France
[2] School of Materials Science and Technology, Institute of Technology, Banaras Hindu University, Varanasi-221005, India

Received 16 November 2001
Published 15 February 2002
Online at stacks.iop.org/JPhysCM/14/2079

Abstract

The room-temperature Raman spectra of $Sr_{1-x}Ca_xTiO_3$ (SCT) for $x = 0.06$ (SCT06), 0.12 (SCT12) and 0.30 (SCT30) are shown to contain first-order Raman lines corresponding to E_g and B_{1g} modes, which appear below 105 K in pure $SrTiO_3$. The E_g line shows slight asymmetry, indicating the orthorhombic structure of SCT for $x \geqslant 0.06$. The low-temperature Raman spectra of SCT06 and SCT12 contain Raman-active modes of symmetry B_{2g} and E_g, predicted by group theory but not observed in $SrTiO_3$ or SCT0.7 ($x = 0.007$) by previous workers. The polar hard modes TO_2 (175 cm^{-1}) and TO_4 (550 cm^{-1}) are present even at room temperature for SCT06 and SCT12 due to Ca^{2+}-centred ferroelectric microregions. The intensity of these modes starts increasing below 55 and 80 K for SCT06 and SCT12 respectively, which are nearly 2 T_c, where T_c is the temperature of the smeared dielectric peak. The presence of such an extended precursor region is akin to relaxor behaviour. For SCT30, two new lines at 79 and 128 cm^{-1} appear below the paraelectric to antiferroelectric phase transition temperature of 230 K. It is shown that Raman lines characteristic of both ferroelectric and antiferroelectric phases are present in SCT12 below 100 K, confirming the frustration model for the highly smeared dielectric response for this composition.

1. Introduction

The solid solution system $Sr_{1-x}Ca_xTiO_3$ (SCT) has received considerable attention in recent years [1–9]. Both the end members, i.e. $SrTiO_3$ (ST) and $CaTiO_3$ (CT), are known to be quantum paraelectrics [10, 11]. Bednorz and Muller [12] have shown that Ca^{2+} doping of ST

[3] Author to whom any correspondence should be addressed.

0953-8984/02/082079+14$30.00

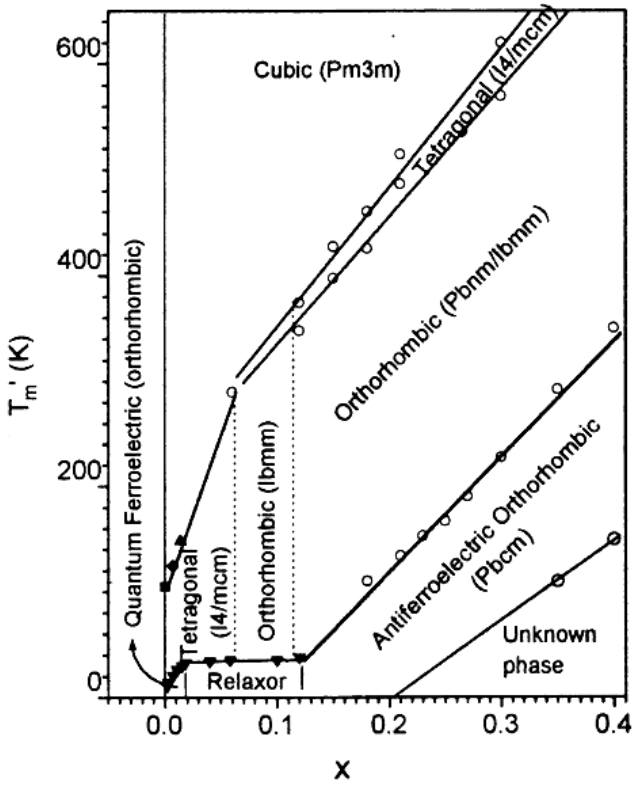

Figure 1. Phase diagram of the SCT system after Ranjan *et al* [1, 2].

can stabilize a quantum ferroelectric phase in the SCT system above a critical concentration ($x_c = 0.0018$) at low temperatures (<40 K). On increasing the Ca^{2+} concentration beyond $x \approx 0.016$, the peak in the dielectric constant (ε') versus temperature (T) plots becomes increasingly smeared out, akin to relaxor ferroelectrics (RFEs). Ranjan *et al* [2] have recently proposed that this smearing is a result of frustration due to competing ferroelectric and antiferroelectric (AFE) instabilities in the system. The recent discovery by Ranjan *et al* [1,2] of an AFE phase transition in SCT for $0.12 < x \leqslant 0.40$ lends credence to the frustration model.

Ranjan and Pandey [1] have proposed a new phase diagram for this system for the composition range $0 \leqslant x \leqslant 0.40$, which is given in figure 1. It is evident from this phase diagram that the system possesses a rich variety of phases in different x–T regimes. At room temperature the structure of SCT is cubic up to $x < 0.06$, beyond which it becomes non-cubic. For $x \geqslant 0.12$, the experimental evidence supports an orthorhombic structure of SCT [3]. A variety of phases showing quantum paraelectric [10], quantum ferroelectric [12], RFE and AFE [2] behaviours are stabilized at low temperatures for $0 \leqslant x < 0.002, 0.002 \leqslant x \leqslant 0.016, 0.016 \leqslant x \leqslant 0.12$ and $0.12 < x \leqslant 0.35$ compositions, respectively. In addition to these phase transitions, there are antiferrodistortive (AFD) phase transitions involving R- and M-point instabilities. For $0 \leqslant x < 0.06$, the cubic–tetragonal AFD transition is driven by the R-point instability [6, 9, 13]. For $x > 0.06$, the cubic–tetragonal–orthorhombic sequence of AFD transitions involves both R- and M-point instabilities [3]. Further, there is an 'unknown' phase for $0.20 \leqslant x \leqslant 0.40$, to which the AFE phase transforms on lowering the temperature.

Raman scattering studies have been very useful in unravelling the structural AFD and ferroelectric phase transitions in pure as well as lightly Ca^{2+}-doped ST [9, 13]. There is no Raman scattering study for the RFE region and the AFE region of the phase diagram. We report here the results of Raman investigations on three SCT compositions representative of RFE ($x = 0.06$, i.e. SCT06), AFE ($x = 0.30$, i.e. SCT30) and a border-line composition ($x = 0.12$, i.e. SCT12) between RFE and AFE. We have also included our results on pure ST for ready comparison with those on the three SCT compositions. A brief report on the Raman scattering studies on the SCT30 composition has been published recently [14].

2. Experiment

Sintered ceramic specimens of SCT with $x = 0.06, 0.12$ and 0.30 were prepared by the conventional solid-state route, the details of which are given in [3]. Raman scattering experiments were performed on a single crystal of ST, and on sintered pellets of SCT06, SCT12 and SCT30. One face of the pellets was mirror polished with diamond paste. The spectra were recorded on a Raman double monochromator (CODERG) with $\lambda = 514.5$ nm. To avoid the thermal effect, the laser power was kept lower than 100 mW. To avoid high parasitical light due to the spot laser size on the pellet, we used a low-angle laser excitation. The Raman bands were recorded using a spectral resolution of $\Delta\nu = 2\ \mathrm{cm}^{-1}$. For calculating the integral intensities of Raman bands we used the software Spectra Max 32 for Windows. During the low-temperature measurements the sample was mounted in an optical cryostat from SMC Instruments. Temperature was controlled and monitored using calibrated Si diodes.

3. Results and discussion

3.1. Phase transitions in pure $SrTiO_3$

At room temperature and normal pressure, ST has an ideal cubic perovskite structure with space group *Pm3m* (O_h^1). The five atoms in the primitive unit cell are located at a point of inversion symmetry. The Raman spectrum at room temperature is therefore restricted to second-order scattering only [15]. At the Brillouin zone centre, the 15 degrees of freedom lead to one $F_{1u}(\Gamma_{15})$ triply degenerate acoustic mode, three $F_{1u}(\Gamma_{15})$ optical modes and one $F_{2u}(\Gamma_{25})$ optical mode. One of the F_{1u} optical modes plays a preponderant role in the incipient ferroelectric behaviour of ST at low temperature and is called the ferroelectric soft mode [16]. The phonon mode important in the description of the cubic–tetragonal structural phase transition of ST is the $F_{2u}(\Gamma_{25})$ mode located at the R symmetry point of the cubic Brillouin zone boundary with wavevector $(1/2, 1/2, 1/2)$ [16]. Since neither the F_{1u} mode at the centre of the Brillouin zone nor the F_{2u} mode at the R-point of the zone boundary are Raman active, the Raman spectra of the cubic phase (see figure 2) mainly reveal two broad bands around 300 and 650 cm^{-1} involving the combination of two phonons (second-order Raman spectrum) [15, 17]. At wavenumber lower than 200 cm^{-1}, only a broad band around $\nu = 79\ \mathrm{cm}^{-1}$ emerges from the background.

On cooling below 300 K, two shoulders, one on each side of the $\nu = 79\ \mathrm{cm}^{-1}$ band, appear around $\nu \approx 40$ and 120 cm^{-1} at 115 K in figure 2. These two shoulders present a decreasing Raman shift as temperature is lowered. It has been shown that these Raman structures are the signature of ferroelectric microordered regions (FMR) induced by polar dopant impurities in the cubic phase of the compound [15, 18]. In our samples, the relative concentrations of impurities (in ppm) are Al 10, Ca 14 and Ba 19. In the FMR regions, the triply degenerate ferroelectric F_{1u} soft mode is split into longitudinal (LO) and transverse optical (TO) modes by the distortion of the unit cell, which breaks the crystal inversion symmetry. By performing electric-field-

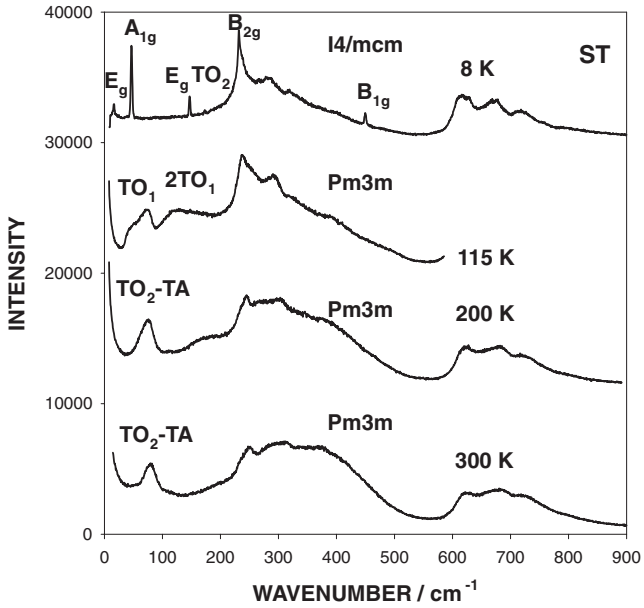

Figure 2. Raman spectra of a pure strontium titanate single crystal with cubic faces [100] in scattering geometry $x(z,(z,x))y$.

induced Raman scattering in ST, Fleury and Worlock [13] have measured the frequencies of the TO_1, TO_2 and TO_4 phonons occurring from this process at 44 cm^{-1} ($T = 85$ K), 173 and 560 cm^{-1} ($T = 47$ K) respectively. Following Bianchi *et al* [9], the first shoulder ($\nu \approx 40\,cm^{-1}$ at 115 K) corresponds to first-order Raman scattering from the TO_1 mode, the other shoulder ($\nu \approx 120$ cm^{-1} at 115 K) to second-order Raman scattering from $2TO_1$ sum modes and the $\nu \approx 79$ cm^{-1} band is attributed to scattering from TO_2–TO_1 or TO_2–TA difference modes.

The cubic–tetragonal AFD phase transition at 105 K originates from the tilting of TiO_6 octahedra in such a way that we have an 'antiphase' rotation of these octahedra in successive layers along one cubic axis. This modification is described in the Glazer classification [19] by the $a^0a^0c^-$ tilt system. The final result is a tetragonal $I4/mcm$ structure (D_{4h}^{18}) with two ST molecular units in the primitive unit cell. Seven Raman-active modes are expected from factor group analysis for the $I4/mcm$ space group with two molecular units in the primitive cell:

$$\Gamma(\text{vib.}) = A_{1g} + B_{1g} + 2B_{2g} + 3E_g.$$

The main signature of the tetragonal phase results from the lifting of the degeneracy of the F_{2u} soft mode, which provides the two Raman-active modes of symmetry E_g and A_{1g} (see the 8 K patterns in figure 2). These lines harden upon cooling due to an increase of the rotation angle of the TiO_6 octahedra. Their frequencies grow from 0 to 46 cm^{-1} (A_{1g}) and 16 cm^{-1} (E_g) as $T \to 8$ K (see figure 3). The other characteristic modes at this temperature are the E_g mode (146 cm^{-1}), the B_{1g} mode (450 cm^{-1}) and the B_{2g} mode (232 cm^{-1}).

It is well known that the soft ferroelectric F_{1u} mode (of unresolved $A_{2u} + E_u$ components in the tetragonal phase [20]) and the AFD F_{2u} mode ($E_g + A_{1g}$ in the tetragonal phase) intersect at 70 K (for the A_{1g} mode) and $T = 40$ K (for the E_g mode). The phonon frequencies of these crossings are ≈40 and 16 cm^{-1} respectively. The low-energy crossing at 40 K and its correlation with phonon anomalies has been accurately discussed in several papers [21, 22]. Our Raman spectra have also revealed two anomalies in the Raman intensity around $T = 70$

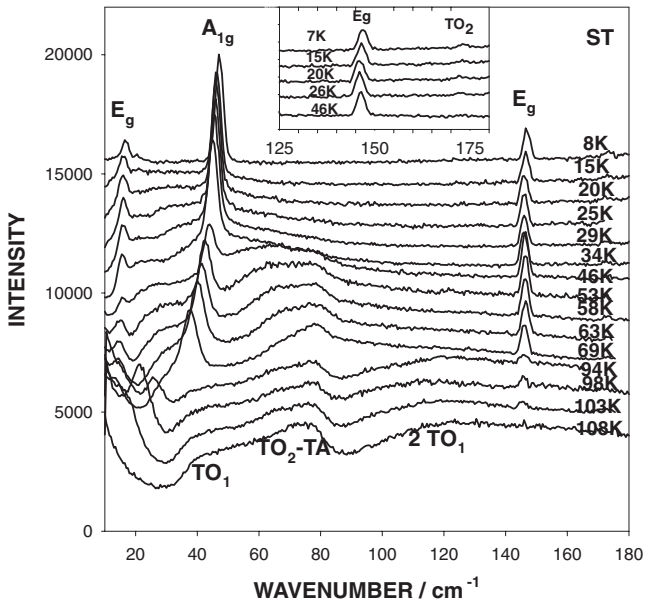

Figure 3. Raman spectra of pure strontium titanate in the tetragonal phase recorded up to 180 cm^{-1} between 8 and 108 K. The Raman spectra reveal two anomalies in the Raman intensity around $T = 40$ and 70 K.

and 40 K in the low-energy region (figure 3). On lowering the temperature, an abrupt increase of intensity of the E_g mode (150 cm^{-1}) was observed at $T \approx 70$ K. Further, the broad band around 75 cm^{-1} on the high-energy side of the A_{1g} mode (the TO_2–TO_1 or TO_2–TA band) disappeared rapidly on approaching $T = 35$ K (see figure 3). However, there is no signature of a modification of the tetragonal structure below 35 K.

It has been shown that on cooling down to 1.5 K there is no evidence for a structural phase transition or a local frozen polar ordering [23]. This is believed to be due to quantum fluctuations which suppress the incipient ferroelectricity of ST at very low temperature [10] by stabilizing the F_{1u} soft mode at $T \leqslant 20$ K. In our Raman spectra of ST at very low temperatures, there is the appearance of the TO_2 polar hard mode ($\nu = 173$ cm^{-1}) and its slight increase in intensity on lowering the temperature from $T = 20$ to 8 K (see inset in figure 3). The appearance of the TO_2 polar mode is due to the FMRs centred around the impurity atoms in our ST single crystal. The fact that the intensity of the hard TO_2 mode increases only marginally suggests that the FMRs do not grow enough to lead to a percolative-type ferroelectric phase transition [9] on account of insufficient concentration of impurities in our ST crystal.

3.2. Relaxor ferroelectric transition in $Sr_{0.94}Ca_{0.06}TiO_3$

In the SCT system, the AFD transition temperature increases with increasing Ca^{2+} content [2]. For example, for $x = 0.007$, it has been shown [9] that the structural soft E_g ($\sim$14 cm^{-1}) and A_{1g} ($\sim$52 cm^{-1}) modes, similar to those in ST below 105 K [15] shown in figure 3, appear below 125 K, signalling the cubic–tetragonal AFD transition. The Raman spectra for SCT06 at 300, 200, 100 and 8 K are depicted in figure 4. The presence of the first-order hard structural E_g ($\sim$145 cm^{-1}) mode even at room temperature, similar to that observed in the low-temperature tetragonal phase of ST (<105 K) or SCT0.7 ($x = 0.007$) (<125 K), clearly

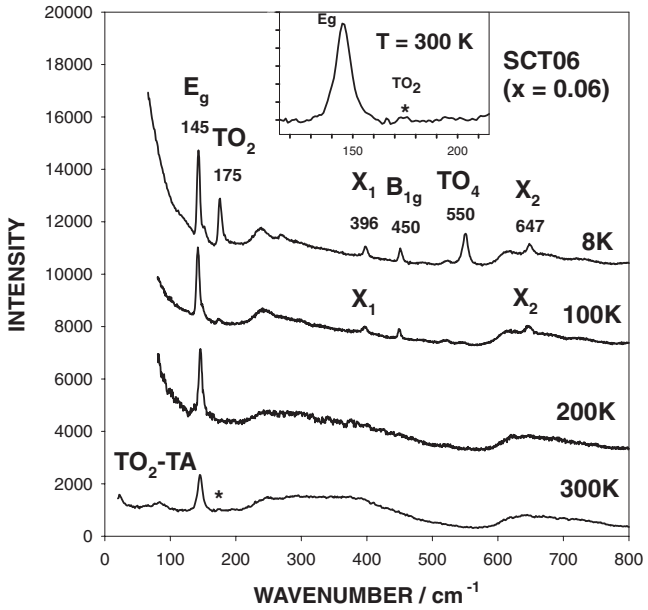

Figure 4. The Raman spectra of $Sr_{0.94}Ca_{0.06}TiO_3$ (SCT06) at various temperatures.

suggests the non-cubic structure of SCT06 even at room temperature (i.e. 300 K). A very careful XRD study of different SCT compositions has indeed revealed non-cubic structure for $x > 0.550$ [4]. The two broad bands in the 300 K spectra centred around 300 and 650 cm^{-1} are superpositions of different combination modes similar to those in pure ST and SCT0.7 [9, 15]. Further, the scattering band around 73 cm^{-1} is due to the TO_2–TO_1 or TO_2–TA difference mode [9]. On lowering the temperature, the difference band disappears as can be seen from the spectra for $T = 100$ K. Further, the intensity of the two high-frequency ($\sim$300 and 600 cm^{-1}) second-order scattering bands decreases substantially. In addition, new bands, marked as X_1 and X_2 in figure 4, have appeared at 396 and 647 cm^{-1} besides the structural B_{1g} hard mode at $\sim$ 450 cm^{-1}. We suspect the X_1 and X_2 to be Raman-active modes of symmetry B_{2g} and E_g predicted by group theory for the tetragonal $I4/mcm$ structure but not observed so far in either ST or SCT0.7.

We are unable to see the soft structural mode due to large diffuse scattering from the ceramic pellet. For the low-temperature tetragonal phase of ST and SCT0.7 the structural E_g mode is represented by a symmetric profile [9, 15]. The structural E_g mode in figure 4, on the other hand, shows an asymmetric tail even at 300 K, as shown more clearly in the inset. This asymmetry becomes more prominent at lower temperatures (see the 100 K pattern). This observation cannot be reconciled with the results of neutron diffraction studies about the tetragonal (space group $I4/mcm$) structure of SCT06 just below 300 K [3] and points towards the possibility of a weak orthorhombic distortion of SCT06 structure around 300 K and below. This weak orthorhombic distortion is most likely due to the presence of a double-tilt system i.e. $a^-a^-c^0$ in terms of Glazer's notation [19]. Since in the phase diagram shown in figure 1 the SCT06 composition sits at the borderline of the tetragonal ($I4/mcm$, $a^0a^0c^-$) and orthorhombic (*Ibmm*, $a^-a^-c^0$) regions, this finding is not surprising. A more detailed study is required to determine the temperatures at which the asymmetry of the E_g mode disappears leading to orthorhombic–tetragonal phase transition. The E_g mode will eventually disappear when the

tetragonal structure transforms to cubic at still higher temperatures. The CT end [24] and SCT compositions with $x \geqslant 0.12$ [3] exhibit the orthorhombic–tetragonal–cubic sequence of phase transitions as confirmed by XRD studies but no such study exists for $x < 0.12$. Our Raman results reveal that the above sequence of phase transitions may continue even up to $x = 0.06$.

Dielectric measurements of Bednorz and Muller [12] have shown a very diffuse and much sharper transition with permittivity maximum at 35 and 18 K for SCT06 and SCT0.7 respectively. It has been argued that these transitions are mediated by ferroelectric microregions formed around off-centred Ca^{2+} ions [9]. These FMRs grow with decreasing temperature due to the softening of the optical modes until they start overlapping, leading to a percolative-type ferroelectric phase transition [8, 9]. Conclusive evidence in favour of the growth of FMRs leading to a ferroelectric/RFE/dipole glass transition has been obtained in $KTa_{1-x}Nb_xO_3$ (KTN) and $K_{1-x}Li_xTaO_3$ (KLT) [25] systems from a study of the evolution of the intensity of the hard optic modes, TO_2 and TO_3. Since TO_3 is a silent mode [13] in the SCT system, Bianchi *et al* have monitored the evolution of the hard TO_2 and TO_4 modes, whose intensity starts growing a few degrees above T_c and settles down just below T_c to a plateau. However, in marked contrast to KTN and SCT0.7, the hard TO_2 mode ($\sim$175 cm^{-1}) is present even at 300 K, which is $\sim 10T_c$ (marked with an asterisk in figure 4 and shown more clearly in the inset). On lowering the temperature, the hard TO_4 mode ($\sim$550 cm^{-1}) also becomes visible (see the 100 K spectra in figure 4). Further, the profile shape of the TO_2 mode shows typical Fano asymmetry [26]. The intensity of both TO_2 and TO_4 modes, after remaining constant up to about 80 K, starts growing as can be seen from figure 5, which depicts the evolution of the Raman spectra in the 100–600 cm^{-1} range at close temperature intervals for $T < 80$ K. The intensity of the TO_2 and TO_4 modes starts growing at $\sim 2T_c$ and continues to grow even below the permittivity maximum temperature ($T_c \approx 35$ K). Figure 6 depicts the temperature dependence of the integral intensities (corrected for the Bose factor) of the TO_2 and TO_4 bands normalized with respect to that of the B_{1g}($\sim$ 450 cm^{-1}) mode. As pointed out in [26], these data reflect the temperature dependence of the autocorrelation function $\langle P^2 \rangle$ of the spatially (r) and temporally (t) fluctuating Ca^{2+}-induced polarization $P(r, t)$. Our results thus suggest that the FMRs induced by a symmetry breaking defect such as Ca^{2+} are present at $T \approx 10\ T_c$ and start growing below 80 K, which is $\sim 2T_c$. The maximum size up to which these FMRs can grow will be limited by the average separation of 6.5 nm between the neighbouring Ca^{2+} ions in SCT06. The formation of precursor ferroelectric clusters or FMRs at $T \gg T_c$ and their growth below 80 K, which is well above the permittivity maximum temperature ($\sim$35 K), is akin to the RFE [27] or dipole glass [28] transition. It is definitely not like that for regular ferroelectric phase transitions for which the precursor region is not so widely extended. For regular ferroelectrics, the intensity of the TO_2 and TO_4 modes should increase abruptly and eventually exhibit saturation as has been reported for SCT0.7 [9].

Below the paraelectric–ferroelectric phase transition temperature of 18 K [9] in SCT0.7, the triply degenerate soft TO_1 polar mode splits into three lines while the doubly degenerate soft structural E_g mode splits into two lines. As said earlier, we are unable to see the soft TO_1 and E_g modes due to large diffuse scattering from the SCT06 pellet surface in the low-wavenumber region. Further, in marked contrast to SCT0.7, the structural E_g mode in SCT06 shows an asymmetric tail even at 300 K due to the orthorhombic distortion corresponding to the $a^-a^-c^0$ tilt system. On cooling below 80 K, this asymmetric profile splits into two clear lines as can be seen from figure 5. We feel that with the growth of the Ca^{2+}-centred FMRs below 80 K, as evidenced by the increase in the intensity of the TO_2 and TO_4 lines, there is additional orthorhombic distortion related to the local polar ordering. This is quite distinct from and is in addition to the orthorhombic distortion above 80 K due to the $a^-a^-c^0$ tilt system.

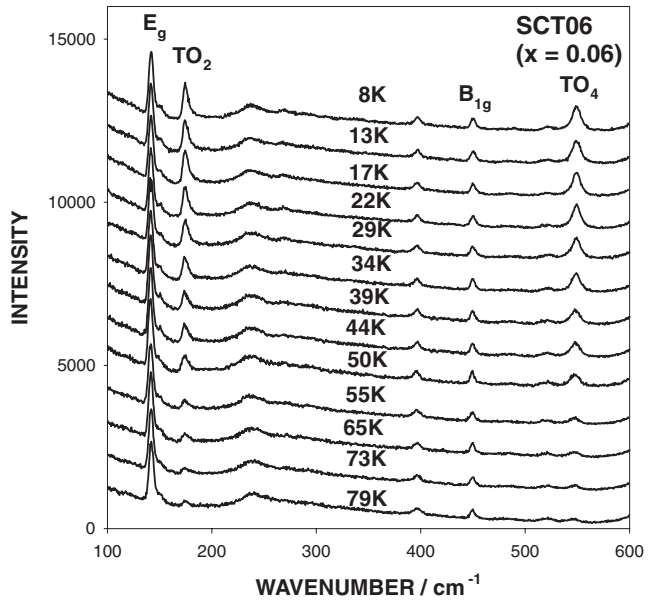

Figure 5. Evolution of the Raman spectra of $Sr_{0.94}Ca_{0.06}TiO_3$ (SCT06) in the temperature range 8–79 K. Note the strong enhancement in intensity of the TO_2 and TO_4 hard polar modes below $T = 55$ K.

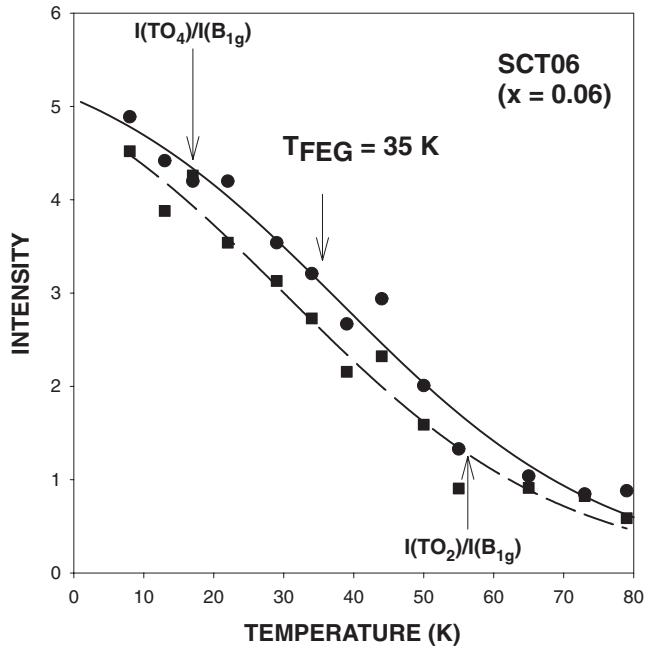

Figure 6. $Sr_{0.94}Ca_{0.06}TiO_3$ (SCT06): temperature dependence of the integral intensity of the TO_2 and TO_4 modes occurring around 170 and 541 cm^{-1} respectively, with respect to the integral intensity of the B_{1g} mode (450 cm^{-1}).

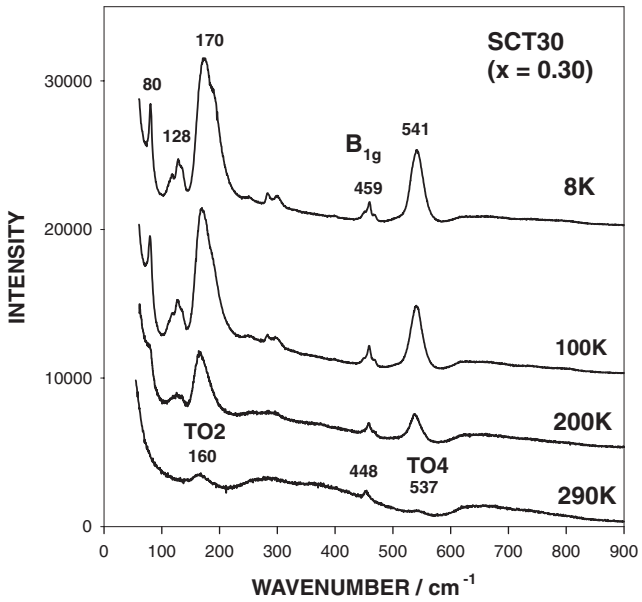

Figure 7. Raman spectra of $Sr_{0.70}Ca_{0.30}TiO_3$ (SCT30) recorded at various temperatures.

3.3. Antiferroelectric transition in $Sr_{0.70}Ca_{0.30}TiO_3$

SCT30 belongs to the orthorhombic *Ibmm* (D_{2h}^{28}) space group at room temperature (300 K) [1]. Figure 7 depicts the Raman spectra of SCT30 recorded at 290, 200, 100 and 8 K. The two broad bands in the 290 K spectra centred around 300 and 650 cm^{-1} are easily recognizable as being due to the second-order Raman scattering. The hard E_g ($\sim$145 cm^{-1}) mode is also embedded in figure 7 in the broad band centred around 160 cm^{-1} at 290 K. Similarly, the hard B_{1g} ($\sim$ 448 cm^{-1}) and another line near the TO_4 band ($\sim$537 cm^{-1}) are also clearly seen at room temperature. All these confirm the non-cubic structure of SCT30 at 290 K. However, the orthorhombic splitting of the E_g line is not discernible due to large Sr–Ca disorder effects [29].

In the Raman spectra recorded at 200 K and below, new lines become visible along with a drastic decrease in the intensity of the second-order Raman bands. To determine the exact temperature at which one observes this modification of the Raman spectra, we depict in figure 8 the evolution of the Raman spectra at close temperature intervals from 296 to 206 K. It is evident from this figure that two new lines around 79 and 128 cm^{-1} appear at $T \leqslant 236$ K. Concomitantly, there is a sudden enhancement in the intensity of the modes near 161 and 537 cm^{-1} at 300 K. In addition, the intensity of the hard B_{1g} ($\sim$ 448 cm^{-1} at 300 K) mode also starts increasing marginally around 236 K. Further, the Raman bands centred around 161, 448 and 537 cm^{-1} at 300 K shift to 170, 459 and 541 cm^{-1} respectively at 100 K.

Since the paraelectric to AFE phase transition in SCT30 occurs around 230 K [2], the strong modification of the Raman spectra below 236 K is obviously linked with this transition. The paraelectric and AFE phases of SCT30 belong to the *Ibmm* (D_{2h}^{28}) and *Pbma* (D_{2h}^{11}) (or equivalently *Pbcm* in a different setting) space groups, respectively [1]. If we neglect the disorder due to the Sr–Ca substitution, 24 Raman-active modes are expected from factor group analysis for the *Ibmm* space group with four molecular units in the primitive cell:

$$\Gamma(\text{vib.}) = 4A_g + 6B_{1g} + 6B_{2g} + 8B_{3g}.$$

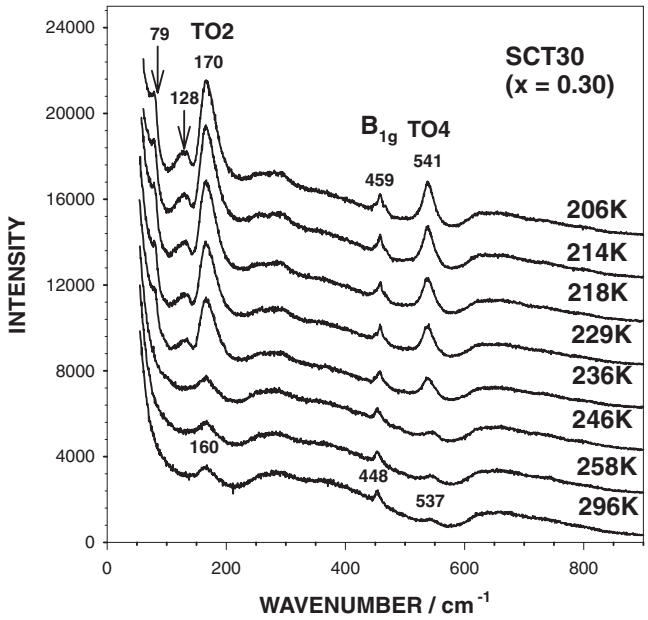

Figure 8. The evolution of the Raman spectra of $Sr_{0.70}Ca_{0.30}TiO_3$ SCT30 as a function of temperature from 206 to 296 K. The two new spectral bands appearing around $T = 236$ K are marked with arrows.

In the *Pbma* space group with eight molecular formula units in the primitive cell, one expects 60 Raman-active modes, neglecting of course the Sr–Ca disorder effects:

$$\Gamma(\text{vib.}) = 15A_g + 15B_{1g} + 15B_{2g} + 15B_{3g}.$$

The appearance of effectively many more bands in the Raman spectra of SCT30 below 236 K in figures 7 and 8 is therefore very much expected with the change of space group accompanying the phase transition. The two new Raman lines occurring around 79 and 128 cm^{-1} in the AFE phase of SCT30 are not present in the ferroelectric phase of SCT0.7 or the RFE phase of SCT06. Since AFE phase transitions are driven by $q \neq 0$ phonons [30], the new modes are due to such $q \neq 0$ phonons. The $q \neq 0$ phonons have become Raman active due to the folding of the corresponding special points into the zone centre below the cell-doubling AFE transition temperature. Further, the sudden enhancement of intensity of the lines near TO_2 and TO_4 positions of SCT0.7 and SCT06 at the paraelectric–AFE phase transition temperature suggests that even these lines in the SCT30 sample are not due to the zone centre ($q = 0$) phonons but correspond to phonons of symmetry points with $q \neq 0$ in the Brillouin zone [30] which become Raman active below the AFE phase transition temperature. Their presence, with considerably subdued intensity, in the paraelectric phase of SCT30 may be mediated by the Sr–Ca disorder, which may relax the wavevector selection rule such that the contributions from phonons at symmetry points with $q \neq 0$ in the Brillouin zone may also become observable in the Raman spectra.

As per the phase diagram given in figure 1, the AFE phase of SCT30 should transform into another unknown type phase around 80 K. In the temperature dependence of the integral intensity of the bands near 170 and 541 cm^{-1} shown in figure 9, there is indeed a change of slope at two temperatures, namely 235 and 80 K respectively. The first change of slope, occurring around 235 K, correlates very well with the AFE phase transition temperature [2]. The onset of a second change of slope around 80 K nearly coincides with the second phase

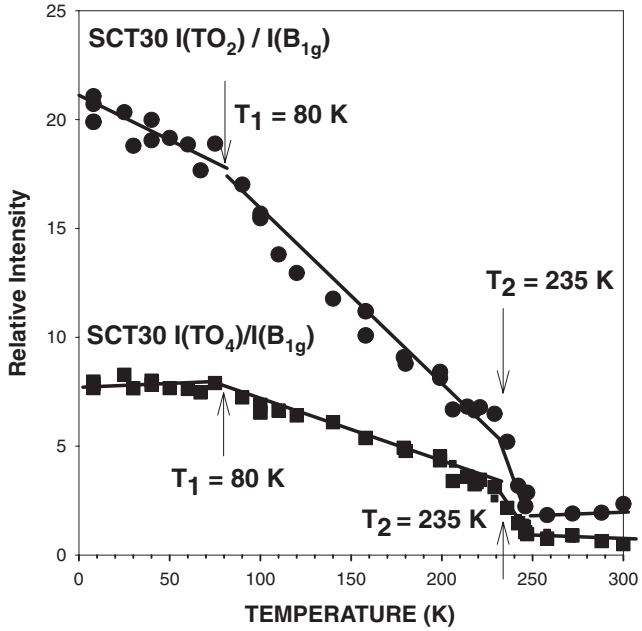

Figure 9. $Sr_{0.70}Ca_{0.30}TiO_3$ (SCT30): temperature dependence of the ratio of the integral intensity of the spectral bands occurring around 170 cm^{-1} (circles) and 541 cm^{-1} (squares) to the integral intensity of the B_{1g} mode. The changes of slope around 235 and 80 K are clearly visible.

transition temperature into the unknown type of phase, predicted by Ranjan *et al* [2] in their phase diagram. As a result of the second transition, the broad band centred around 170 cm^{-1} at $T = 235$ K (see figure 8) splits into two peaks centred around 170 and 190 cm^{-1} at $T = 8$ K as can be seen from figure 7. The lines present at 8 K in the frequency range 50–600 cm^{-1} are as follows: 80, 116, 128, 135, 170, 190, 249, 284, 300, 451, 459, 469 and 541 cm^{-1}.

3.4. Evidence for competing ferroelectric and antiferroelectric interactions in $Sr_{0.88}Ca_{0.12}TiO_3$

The temperature evolution of the Raman spectra for SCT12 in the 300–8 K range shown in figure 10 has mixed features common to both SCT06 and SCT30. SCT12 has been shown to be orthorhombic [4] at room temperature since it undergoes two tilt transitions [3]. At first appearance, the Raman spectra of SCT12 and SCT06 are similar at 300 K. As in SCT06, the Raman spectrum of SCT12 shows two bands at 80 and 145 cm^{-1}, localized at the frequencies of the TO_2–TA and the E_g bands, respectively. In addition, it shows large structureless second-order Raman scattering at higher wavenumbers.

Since most of the Raman-active modes, which would appear in the orthorhombic phase, arise from Raman-inactive u modes of the tetragonal phase, one expects only weak signals for these modes such as asymmetry of the E_g band at 300 K, which is present in the room-temperature spectra.

On cooling the sample, the intensity of the second-order Raman scattering strongly decreases. More importantly, the asymmetric E_g band at 300 K shows clear splitting ($\Delta\nu \approx 11$ cm^{-1}) at lower temperature ($\leqslant$100 K) in confirmation of the orthorhombic structure, which lifts the E_g degeneracy. As in SCT06, the B_{2g} and E_g modes at 398 and 648 cm^{-1} are also present in the $T \leqslant 100$ K spectra. On lowering the temperature below 100 K, there is

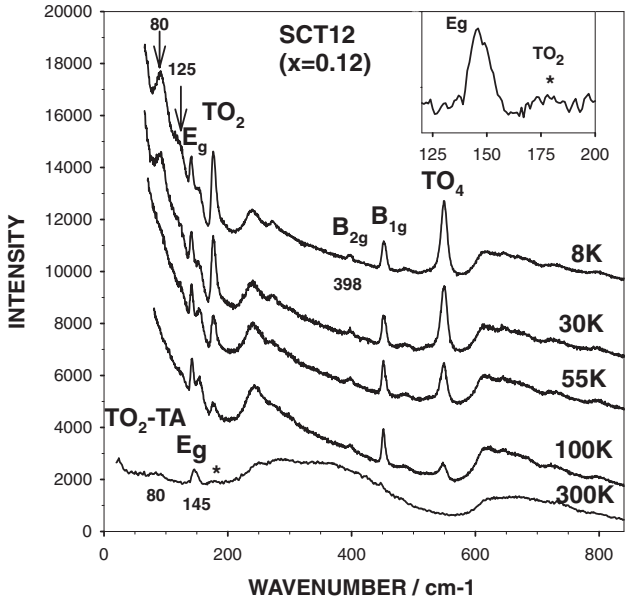

Figure 10. The evolution of the Raman spectra of $Sr_{0.88}Ca_{0.12}TiO_3$ (SCT12) as a function of temperature from 8 to 300 K.

a marked enhancement in the intensities of TO_2 and TO_4 modes, which may be attributed to the growth of Ca^{2+}-centred FMRs. The rise of intensity of these modes is less steep than that for lower Ca^{2+} (e.g. $x = 0.06$) content, as can be seen from a comparison of figure 11 with 6. The enhancement in the intensity of the TO_2 and TO_4 bands clearly indicates that the growth of the FMRs starts well above the dielectric constant peak temperature (∼38 K) [12], similar to what is expected for RFE [27]. The structural E_g mode persists down to 8 K and its splitting increases with decreasing temperature, similar to the case of the FE and RFE phases of SCT0.7 and SCT06 respectively, but, intriguingly, new modes around 80 and 125 cm^{-1}, similar to those in the AFE phase of SCT30, also appear at $T \leqslant 100$ K. We have already seen in the SCT30 context that these two modes are characteristic of AFE correlations. Our Raman scattering studies thus indicate the coexistence of FE and AFE instabilities in SCT12.

The dielectric studies suggest that the FE and AFE interactions dominate for $0.0018 \leqslant x \leqslant 0.016$ and $0.12 < x \leqslant 0.40$ compositions. For the intermediate composition range $0.016 < x \leqslant 0.12$, the two types of interaction frustrate each other, leading to smeared dielectric response as was first pointed out by Ranjan *et al* [2]. Even in the frustrated regime ($0.016 < x \leqslant 0.12$), one expects dominant FE interactions towards the Sr^{2+}-rich end and dominant AFE interactions at the Ca^{2+}-rich end. Ranjan *et al* accordingly proposed that there should be a crossover from RFE to relaxor AFE-type response around $x = 0.10$. Our Raman studies confirm this prediction since SCT06 shows ferroelectric modes while SCT12 exhibits both ferroelectric and AFE modes at low temperatures. The present work seems to be the first direct evidence for the presence of frustration in disordered perovskites.

4. Conclusions

The Raman spectra of SCT06, SCT12 and SCT30 at 300 K contain first-order Raman lines corresponding to E_g and B_{1g} modes of the low-temperature ($T < 105$ K) phase of ST. The E_g line shows slight asymmetry, confirming the orthorhombic structure of SCT for $x \geqslant 0.06$.

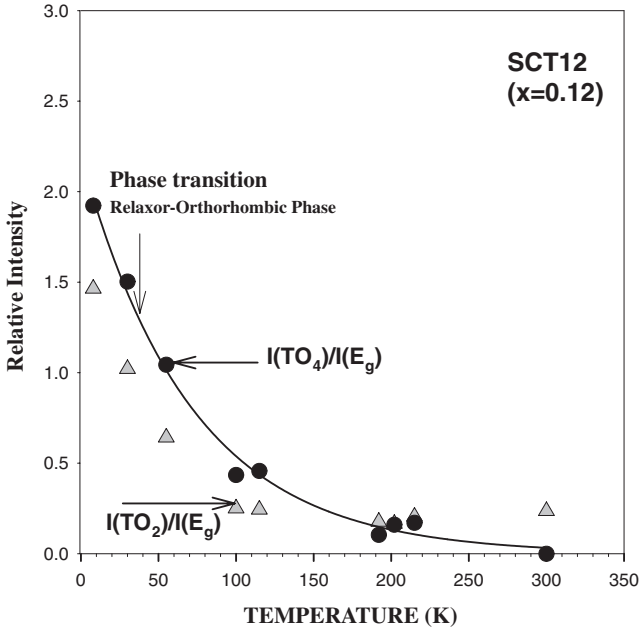

Figure 11. Temperature dependence of the integral intensity of the 175 cm^{-1} band (triangles) and of the 550 cm^{-1} band (circles) with respect to the integral intensity of the 145 cm^{-1} E_g for $Sr_{0.88}Ca_{0.12}TiO_3$ (SCT12).

In contrast, the Raman spectra of pure ST at 300 K show only second-order Raman scattering due to its cubic structure.

For pure ST, we confirm the interaction of the soft ferroelectric F_{1u} mode with the A_{1g} and E_g structural modes at 70 and 40 K, respectively. In the low-temperature Raman spectra of SCT06 and SCT12 one observes Raman-active modes of symmetry B_{2g} and E_g, predicted by group theory but not observed in ST and SCT0.7. The polar hard modes TO_2 (175 cm^{-1}) and TO_4 (550 cm^{-1}) are present even at room temperature for SCT06 and SCT12 due to the Ca^{2+}-centred ferroelectric microregions. The intensity of these modes starts increasing below 55 and 80 K for SCT06 and SCT12 respectively, which are nearly $2T_c$, where T_c is the temperature of the smeared dielectric peak. The presence of such an extended precursor region is akin to relaxor behaviour.

For SCT30, two new lines at 79 and 128 cm^{-1} appear below the paraelectric to AFE phase transition temperature, which lies around 230 K. These two lines are attributed to $q \neq 0$ phonon modes of the paraelectric phase and are present even in SCT12 below 100 K. The presence of ferroelectric and AFE modes in SCT12 at $T < 100$ K provides direct evidence for the frustration model for the smearing of the dielectric response proposed by Ranjan *et al* [2].

References

[1] Ranjan R and Pandey D 2001 *J. Phys.: Condens. Matter* **13** 4239
Ranjan R and Pandey D 2001 *J. Phys.: Condens. Matter* **13** 4250
[2] Ranjan R, Pandey D and Lalla N P 2000 *Phys. Rev. Lett.* **84** 3726
[3] Ranjan R, Pandey D, Siruguri V, Krishna P S R and Paranjpe S K 1999 *J. Phys.: Condens. Matter* **11** 2233
Ranjan R and Pandey D 1999 *J. Phys.: Condens. Matter* **11** 2247
[4] Ranjan R, Pandey D, Schuddinck, Richard O, De Meulenaere P, Van Landuyt J and Van Tendeloo G 2001 *J. Solid State Chem.* **162** 20

[5] Howard C J, Withers R L and Kennedy B J 2001 *J. Solid State Chem.* **160** 8
[6] Guzhva M E, Lemanov V V and Markovin P A 1997 *Phys. Solid State* **39** 618
[7] Dec J, Kleeman W, Bianchi U and Bednorz J G 1995 *Europhys. Lett.* **29** 31
[8] Kleeman W, Bianchi U, Burgel A, Prasse M and Dec J 1995 *Phase Transitions* **55** 57
Kleeman W, Dec J and Westwanski B 1998 *Phys. Rev.* B **58** 8985
[9] Bianchi U, Kleemann and Bednorz 1994 *J. Phys.: Condens. Matter* **6** 1229
[10] Muller K A and Burkard H 1979 *Phys. Rev.* B **19** 3593
[11] Kim I S, Itoh M and Nakamura T 1992 *J. Solid State Chem.* **101** 77
[12] Bednorz J G and Muller K A 1984 *Phys. Rev. Lett.* **52** 2289
[13] Fleury P A and Worlock J M 1968 *Phys. Rev.* B **174** 613
[14] Mishra S K, Ranjan R, Pandey D, Ouillon R, Pinan-Lucare J P, Ranson P and Pruzan Ph 2001 *Phys. Rev.* B **64** 092302
[15] Nilsen W G and Skinner J G 1968 *J. Chem. Phys.* **48** 2240
[16] Cowley R A 1964 *Phys. Rev.* **134** A981
Cowley R A 1962 *Phys. Rev. Lett.* **9** 159
[17] Sekine K T, Uchinokura and Matsuura E 1976 *Solid State Commun.* **18** 569
[18] Uwe H, Ymagushi H and Sakudo T 1989 *Ferroelectrics* **96** 123
[19] Glazer A M 1972 *Acta Crystallogr.* B **28** 3384
Glazer A M 1975 *Acta Crystallogr.* A **31** 756
[20] Worlock J M, Scott J F and Fleury P A 1969 *Light Scattering Spectra of Solids* ed G B Wright (New York: Springer) p 689
[21] Courtens E, Coddens G, Hennion B, Hehlen B, Pelous J and Vacher R 1993 *Phys. Scr.* T **49** 430
Scott J F 1996 *Ferroelectr. Lett.* **20** 89
[22] Vacher R, Pelous J, Hennion B, Coddens G, Courtens E and Muller K A 1992 *Europhys. Lett.* **17** 45
[23] Kiat J M and Roisnel T 1996 *J. Phys.: Condens. Matter* **8** 3471
[24] Redforn Simson A T 1996 *J. Phys.: Condens. Matter* **8** 8267
[25] Calvi P, Camagni P, Giulotto E and Rollandi L 1996 *Phys. Rev.* B **53** 5240
Toulouse J, DiAntonio P, Vugmeister B E, Wang X M and Knauss L A 1992 *Phys. Rev.* B **68** 232
[26] DiAntonio P, Vugmeister B E, Toulouse J, and Boatner L A 1993 *Phys. Rev.* B **47** 5629
[27] Cross L E 1987 *Ferroelectrics* **76** 24
[28] Maglione M, Hochli U T and Joffrin J 1986 *Phys. Rev. Lett.* **57** 436
[29] Barker A S Jr 1968 *Localized Excitations in Solids* ed R F Wallis (New York: Plenum) p 581
Worlock J M and Porto S P S 1965 *Phys. Rev. Lett.* **15** 697
[30] Blinc R and Zeks B 1974 *Soft Modes in Ferroelectrics and Antiferroelelectrics* (Amsterdam: North-Holland)